Original Paper

Cellular Physiology and Biochemistry

Cell Physiol Biochem 2005;15:77-88

Accepted: October 12, 2004

Atrial Natriuretic Peptide Effects on Intracellular pH Changes and ROS Production in HEPG2 Cells: Role of p38 MAPK and Phospholipase D

Patrizia Morena Baldini[1], Paolo De Vito[1], Daniela Vismara[1], Claudia Bagni[1,3], Francesca Zalfa[1,3], Marilena Minieri[2] and Paolo Di Nardo[2]

[1]Department of Biology, [2]Department of Internal Medicine, Laboratory of Cellular and Molecular Cardiology, University of Rome "Tor Vergata", [3] Institute for Experimental Neurosciences, Fondazione Santa Lucia IRCCS, Rome

Key Words

Atrial Natriuretic Peptide • Sodium hydrogen exchanger • Phospholipase D • Reactive Oxygen Species

Abstract

Aims: The present study was performed to evaluate Atrial Natriuretic Peptide (ANP) effects on intracellular pH, phospholipase D and ROS production and the possible relationship among them in HepG2 cells. Cancer extracellular microenvironment is more acidic than normal tissues and the activation of NHE-1, the only system able to regulate pHi homeostasis in this condition , can represent an important event in cell proliferation and malignant transformation. Methods: The ANP effects on pHi were evaluated by fluorescence spectrometry. The effects on p38 MAPK and ROS production were evaluated by immunoblots and analysis of DCF-DA fluorescence, respectively. RT-PCR analysis and Western blotting were used to determine the ANP effect on mRNA NHE-1 expression and protein levels. PLD-catalyzed conversion of phosphatidylcholine to phosphatydilethanol (PetOH), in the presence of ethanol, was monitored by thin layer chromatography. Results: A significant pHi decrease was observed in ANP-treated HepG2 cells and this effect was paralleled by the enhancement of PLD activity and ROS production. The ANP effect on pHi was coupled to an increased p38 MAPK phosphorylation and a down-regulation of mRNA NHE-1 expression and protein levels. Moreover, the relationship between PLD and ROS production was demonstrated by calphostin-c, a potent inhibitor of PLD. At the same time, all assessed ANP-effects were mediated by NPR-C receptors. Conclusion: Our results indicate that ANP recruits a signal pathway associated with p38 MAPK, NHE-1 and PLD responsible for ROS production, suggesting a possible role for ANP as novel modulator of ROS generation in HepG2 cells.

Introduction

Atrial Natriuretic Peptide (ANP), a cardiovascular hormone mainly secreted by heart atria in response to mechanical stress, besides inducing natriuresis and vasodilation *in vivo* [1, 2], also acts as autocrine/paracrine

KARGER

Fax +41 61 306 12 34
E-Mail karger@karger.ch
www.karger.com

1015-8987/05/0154-0077$22.00/0

Accessible online at:
www.karger.com/journals/net

Dr. P.M. Baldini
Department of Biology, University of Rome "Tor Vergata"
via della Ricerca Scientifica, 00133 Rome (Italy)
Tel. +39-06-72594217, Fax +39-06-72594217
E-Mail baldini@uniroma2.it

factor [3] in different organs, such as kidney, lung, thymus and liver [4-7], under physiological as well as pathophysiologic conditions (e. g., cancer) [8]. ANP promotes its biological effects by interacting with two major types of receptors located on plasma membranes of target cells: NPR-A receptors, which activate the guanylate cyclase (GC)/cGMP system, and NPR-C receptors, which inhibit the adenylate cyclase (AC)/cAMP system [9] or the membrane lipid turnover through the activation of specific phospholipases [10]. Among different biological effects, in hepatoblastoma (HepG2) cells, ANP inhibits cell proliferation through the selective upregulation of the expression of the NPR-C receptors associated with decreased intracellular concentrations of cAMP [11]. Furthermore, ANP can inhibit or stimulate Na^+/H^+ exchanger isoform 1 (NHE-1) depending on cell type [12, 13].

In cancerous tissues, extracellular microenvironment is more acid than in normal tissues [14] and the NHE-1, a plasma membrane protein that exchanges Na^+ and H^+ ions according to their concentration gradients [15], concurs to minimize changes in intracellular pH (pHi) and to maintain tumour cell viability. Signal transduction leading to NHE-1 modulation can involve several mitogen-activated protein (MAP) kinases, including p38 MAP kinase [16]. MAP kinases represent an important component of the intracellular signal transduction cascade and regulate a wide range of cell processes including gene transcription, cytoskeletal organization, cell growth and ion homeostasis [17].

Previous reports [18, 19] have suggested that ANP plays a dual role on p38 MAP kinases, inhibiting or stimulating the enzyme activity depending on cell types. In addition, pHi changes in response to a variety of biologically active molecules may act as signaling events regulating different downstream effectors including phospholipase D (PLD) [20], the latter being also activated by ANP at early and long times [21, 22]. PLD catalyzes the hydrolysis of the terminal diester bond of phosphatidylcholine to liberate phosphatidic acid (PA) and choline [23]. A role for PA as key intracellular signaling molecule activating protein kinases, phospholipases and protein tyrosin kinases, has been proposed [24]. Moreover, PA also promotes Reactive Oxygen Species (ROS) production through the NADPH oxidase involvement [25], which, in turn, appears to play a role as cell death mediator in HepG2 cells [26].

Taken together, previous findings suggest a possible relationship among ANP-induced pHi modulation, PLD activation and related downstream signalling systems, such as ROS production. Therefore, the aim of the present study was: (i) to assess the effect of ANP on pHi through the involvement of NHE-1; (ii) to define the role of p38 MAP kinases in ANP-induced pHi modulation; (iii) to establish whether NHE-1 may be responsible for PLD modulation and ROS production in HepG2 cells. The *in vitro* model was selected because, HepG2 cells are highly sensitive to ANP [11] and the NHE-1 exchanger is more active than in normal hepatocytes [27, 28].

Materials and Methods

RPMI 1640, trypsin, glutamine, penicillin (10,000 UI/ml), streptomycin (10,000 μg/ml) and sodium pyruvate were from Eurobio Laboratoires (Le Ulis Cedex, France). Foetal Calf Serum (FCS) was from GIBCO (Grand Island, NY). ANP, ethylenediaminetetraacetic acid tetrasodium salt dehydrate (EDTA), Sodium Dodecyl Sulphate (SDS), Phosphate Buffer Saline (PBS), Triton X100, Dithiotreitol, Mercaptoethanol, Glycerol, Sodium Vanadate, Dimethyl Sulfoxide (DMSO), Pepstatin, Aprotenin, Leupetin, Tris-HCl, Bromophenol blue**,** Phenylmethylsulfonylfluoride (PMFS), N-2-hydorxyethylpiperazine-N'-2-ethanesulfonic acid (HEPES), Ethidium bromide, 8-Br-cGMP, cANF, calphostin-c, monensin, Trypan blue, 5-(N-ethyl-N-isopropyl)-amiloride (EIPA), (3-methylsulphonyl-4-piper-idinobenzoyl)guanidine methanesulphonate) (Hoe-694) were from Sigma Chemicals (St. Louis, MO). 2',7'- dichlorofluorescein diacetate (DCF-DA) and 2'-7' –bis(carboxyethyl)-5(6)-carboxy-fluorescein (BCECF/AM) were from Molecular Probes, Inc. (Eugene, OR). SB203580 and SB202474 were from Calbiochem. Antiphospho- and total p38 kinase and anti sodium-hydrogen exchanger (NHE-1) antibodies were from Santa Cruz Biotechnology (Santa Cruz, CA). Horseradish peroxidase-conjugated secondary antibody and chemiluminescence detection of immunoreactive bands ECL reagents were from Pierce (Rockford, IL). RnaseH, human (NHE-1) primers were from Invitrogen. Taq DNA polymerase, Dnase, (α- ^{32}P) dCTP, [^{3}H]-myristic acid (spec. act. 53 Ci/mmol) were from Amersham, Pharmacia Biotech. Optifluor (Packard Instruments, Downers Grove, IL). Plates for thin layer chromatography and all other chemicals of purest available grade were from Merck (Darmstadt, Germany).

Cell Culture

Hepatoblastoma (HepG2) cell line was purchased from American Type Culture Collection (ATCC, Rockville, MA) and cultured in RPMI-1640 medium supplemented with 10% Foetal Calf Serum (FCS), 4 mM glutamine, 1 mM sodium pyruvate, 100 U/ml penicillin and 100 μg/ml streptomycin. Cells were maintained in a humidified incubator at 37 °C in a 5% CO_2 atmosphere. HepG2 cells, harvested once a week by 0.25% trypsin 0.02% EDTA and re-fed every other day, were used at

about 80% confluence after 4-6 days at passage level 4-10. HepG2 cells were grown in 35 mm dishes and serum starved for 24 h before each experiment to rule out possible interferences with cell growth due to serum components and to promote their synchronization. Cells were adapted to HEPES or Krebs buffer for at least 5 hours before each experiment.

pH measurement

Intracellular pH (pHi) was measured by fluorescence spectrometry using the intracellular probe 2'-7'-bis (carboxyethyl)-5(6)-carboxyfluorescein (BCECF/AM), as previously described [29]. To rule out the contribution of HCO_3^--dependent transport mechanisms, a series of experiments was carried out in a buffer depleted of HCO_3^- with the following composition (mM): 135 NaCl, 1 KCl, 1 $CaCl_2$, 1 $MgCl_2$, 10 glucose, and 20 HEPES, pH 7.4. This buffer (designated HEPES buffer) was used for the incubation with fluorescent probe and the determination of pHi, unless otherwise stated. In order to estimate the role of bicarbonate-dependent transport and keep quiescent the Na^+/H^+ exchanger, a second series of experiments was carried out in Krebs buffer with the following composition (mM): 104 NaCl, 4.7 KCl, 2.5 $CaCl_2$, 1.17 $MgSO_4$, 1.8 KH_2PO_4, 25 $NaHCO_3$, 10 glucose, pH 7.3. Incubation with the fluorescent dye was carried out as follows: cells were washed twice and incubated in either HEPES or Krebs buffer with 1mg/ml fluorescent dye in dimethylsulfoxide (DMSO) at the final concentration of 1μg/ml for 30 min at 37°C in the dark. After incubation, the medium containing the dye was discarded and cells were washed twice with the same buffer. The calibration curve was carried out as previously reported [30] using the nigericin method in high potassium medium with the same composition as the HEPES buffer, but with NaCl substituted by equimolar KCl. The calibration curve was linear in the pH range 6.5-7.5 (not shown). Fluorescence was measured under continuous magnetic stirring at controlled temperature (37°C) in a Perkin-Elmer LS-5 luminescence spectrometer equipped with a chart recorder model R 100A, with excitation and emission wavelengths of 500 nm and 530 nm, using 5 and 10 nm slits, respectively for the two light paths. Fluorescence was also routinely measured at 450 nm excitation (at this wavelength, the fluorescence is proportional to intracellular dye concentration, but is relatively pH insensitive) and the value did not change more than 10% during the experimental period. NHE-1 blocking was obtained with the specific inhibitors 5-(N-ethyl-N-isopropyl)amiloride (EIPA) and (3-methylsulphonyl-4-piper-idinobenzoyl)guanidine methanesulphonate) (Hoe-694) and cell mortality was evaluated by Trypan blue staining using a Neubauer modified chamber. When requested, monensin was used at 10μM final concentration.

Immunoblots

Cells, grown in 6-well plates (10^5 cells/well), were synchronized as reported above and incubated in 2 ml RPMI 1640 without FCS, in the presence or absence of 10^{-10}M ANP for different experimental times. After washing with PBS, cells were centrifuged at 1,500 rpm at 4°C for 5 min and the pellet was lysed with sample buffer containing: 10% sodium dodecyl sulfate (SDS), 10% glycerol, 100 mM dithiotreitol, 5% β-mercaptoetanol, 1% bromophenol blue, 2mM EDTA, 1 mM sodium vanadate, 50 mM Tris-HCl (pH 6.8), plus a cocktail of protease inhibitors (1 mM phenylmethylsulfonylfluoride, 1μg/ml pepstatin, 10 μg/ml leupeptin, 10 μg/ml aprotenin). The lysate was centrifuged at 13,000 rpm for 5 min; the supernatant was boiled for two minutes and then stored at -70°C. The protein content of cell lysates was assessed by the method of Lowry et al. [31]. Equal amounts of whole cell lysate (30-50 ìg) were subjected to 8% (p38 MAPK) and 10% (NHE-1) acrylamide SDS-PAGE, transferred to nitrocellulose membranes, and immunoblotted with primary anti-phosphorylated and total p38 MAP kinase antibodies (both 1:1000) overnight at 4°C or with the primary rabbit polyclonal antibodies for NHE-1 (1:100). A horseradish, peroxidase-conjugated secondary antibodies (1:2500) was used for 1 hour at room temperature. Membranes were counterblotted with 1:5000 dilution of monoclonal anti-β-actin antibodies (Sigma) to ensure same amounts of protein loading on the membranes. Membranes were analyzed by ECL and each experiment was repeated at least three times.

RNA extraction and RT-PCR analysis

Total RNA was extracted from HepG2 cells (about 5 x 10^6) using the single-step method of extraction described by Chomczynski and Sacchi [32]. RNA concentration was determined spectrometrically with a BioPhotometer (Eppendorf, Hamburg, Germany), measuring UV absorbance at 260 nm; the integrity of RNA preparations was assessed by electrophoresis on agarose gel. Total RNA (1 μg) was DNase treated (Amersham Pharmacia Biotech) and reverse-transcribed into cDNA by the random hexanucleotide technique using 100 U of Moloney murine leukemia virus reverse transcriptase (RNaseH) and random primers $p(dN)_6$ (Roche) as previously described [22]. For the RT-PCR analysis, an equal amount (10 pg) of an internal control RNA was added to each sample before reverse transcription. This RNA was obtained by *in vitro* transcription (Ambion, Austin, TX) of the *Xenopus* ribosomal protein L22 sequence (a. n.: X64207) and detected with specific oligonucleotides. An aliquot of RT reaction (2 μl) was PCR-amplified in a final volume of 50 μl by using 200 μM concentration of dATP, dGTP, dTTP and 10 μM of dCTP, 0.5 U of Taq DNA polymerase (Amersham Pharmacia Biotech), 0.2 μCi (α-^{32}P)dCTP (Amersham Pharmacia Biotech; 3000 Ci/mmol) and 20 pmol of each primer designed to amplify the Na/H exchanger1 (NHE1) mRNA coding sequence. The following primes were used based upon the sequence for the human NHE1 mRNA sequence (ID: AF141359); upstream 5'-CCT TCT GAC AGG CAT CGA AG-3', downstream 5'-CCG TCA GGT AGT TGT TGA TCT-3' (fragment size: 470 bp). To normalize the experiments, besides L22 cDNA, the housekeeping cDNA of human β-actin (ID: NM001101) was amplified with the following oligonucleotides: upstream 5'-GCA CTC TTC CAG CCT TCC-3', downstream 5'-GCG CTC AGG AGG AGG AAT-3' (fragment size: 193 bp). All transcripts were amplified as follows: 94°C for 4 min, variable cycles at 94°C for 1 min, 58°C for 1 min and 72°C for 1 min, followed by a final extension at 72°C for 10 min. The number of amplification cycles was preliminarily optimized for

each PCR reaction to avoid saturation (25 cycles for NHE1 and L22 cDNAs and 15 cycles for β-actin cDNA). The amplified fragments were separated on 5% polyacrylamide gel and quantified by the phosphoimager (Molecular Dynamics).

Thin layer chromatography of lipids and transphosphadylation reaction

Preliminary experiments on [^{3}H] myristate incorporation indicated that optimal labeling was at 3h (1μCi/ml). After labeling, cells were left for 1 hour in the medium without FCS and then incubated in HEPES or Krebs buffer. To determine phospholipase D (PLD) activity, different concentrations of ethanol (0.03–1%, v/v) were added to prelabeled cells 15 min before the addition of 10^{-10}M ANP or 10^{-8}M calphostin-c, potent direct and irreversible inhibitor of PLD isoenzyme catalytic domain [33], or 5μM SB203580, inhibitor of p38 MAPK [34]. Incubation was stopped with 1 ml of ice-cold methanol. Cells ($1x10^6$) were scraped off and lipids were extracted by the method of Bligh and Dyer [35]. Dried lipids were redissolved in 20 μl of CH_3Cl. Since the PA produced is rapidly metabolized and could arise from other sources, we measured the formation of PetOH, a widely accepted direct measure of PLD activity [36]. Phosphatidylethanol (PetOH) was separated by thin-layer chromatography on 10x20 cm silica gel 60 plates. The solvent system consisted of ethyl acetate/isooctane/acetic acid/H_2O (130/20/30/100, v/v). After chromatography, plates were dried under N_2 and spots revealed under iodine vapor were scraped off, eluted with 0.2 ml ethanol and counted for radioactivity after the addition of 7 ml Optifluor (Packard Instruments, Downers Grove, IL). PetOH was identified by comparing its Rf value with a standard, according to Chattopadhyay [37].

Detection of ROS in HepG2 cells

Dichlorofluorescein Diacetate (DCF-DA) was dissolved in DMSO at the concentration of 1 mM and kept at -20 °C in the dark; it was freshly diluted before each experiment. Cells ($1x10^6$) were synchronized as reported above, resuspended in PBS buffer and loaded with the fluorescent indicator DCF-DA at the final concentration of 10 μM for 60 min at 37°C in the dark [38]. After the incubation with the fluorescent dye, HepG2 cells were washed twice with PBS buffer, centrifuged for 5 min at 1.500 rpm at room temperature, resuspended in PBS and challenged with ANP; in other experiments, cells were pretreated with different effectors for 1h at 37°C in the dark. A sample of $1x10^5$ cells was used to monitor ROS production. Fluorescence was measured under continuous magnetic stirring and controlled temperature (37°C) in a Perkin-Elmer luminescence spectrometer (model LS-5) equipped with a chart recorder (model R 100A), with excitation wavelength at 485 nm and emission wavelength at 530 nm using 5 and 10 nm slits for each light path, respectively,. Results are expressed as Fluorescence Intensity, reported as Fluorescence Units (F.U.), of cells loaded with only DCF-DA (Control) or also treated with 300 μM H_2O_2 for 1h as positive control.

Statistical analysis

Data distribution was preliminarily verified by the Kolmogorov –Smirnov test. Each experimental set was independently performed and compared with the same control by Student's t-test. The study was not aimed at investigating the potential variability among different experimental sets. Quantitative data are expressed as the mean ± SD of at least four replicate determinations. Differences were regarded as significant when P value was less than 0.5.

Results

Intracellular acidification in HepG2 cells

In order to investigate whether ANP could induce pHi changes in HepG2 cells, a wide concentration range (10^{-11}-10^{-7} M) of natriuretic hormone was used in: (i) HEPES buffer: in order to affect quiescent Na^+-dependent and independent HCO_3^- exchangers and to evaluate the role of NHE-1; (ii) Krebs buffer: to test the role of HCO_3^- exchangers, since both NHE-1 and Na^+-dependent /HCO_3^- are functionally active, but EIPA effects on NHE-1 can be masked by the activation of Na^+-dependent /HCO_3^-. The ANP concentration-response effect on pHi in HepG2 cells is reported in Fig.1. In this regard: (i) in HEPES buffer, the mean average pHi at rest was 7.03±0.03 and 6 hours exposure to low ANP concentrations (10^{-9}-10^{-11}M) significantly reduced pHi which shifted from basal value by 0.36±0.05 pH units, with maximum effect at 10^{-10}M; (ii) in Krebs buffer, the average pHi at rest was 7.07±0.1 and no significant ANP effects were observed with respect to control values (Fig.1, inset).

In Fig.2, the time-course of pHi in the presence of 10^{-10} M ANP is shown. The ANP effect was already significant after 4 hours treatment, while no significant differences were present between 4and 6 hours treatment. For this reason, 10^{-10}M ANP for 6 hours was used in all subsequent experiments.

To further verify whether NHE-1 was involved in ANP-induced pHi decrease, we carried out experiments in HEPES buffer in the presence of 1μM EIPA or 3 μM Hoe-694, specific inhibitors of the exchanger. Fig.3a shows that ANP has the similar acidifying effect as EIPA or Hoe-694, while ANP plus EIPA or ANP plus Hoe-694 has not additive effects. Fig.3b shows that 10 μM monensin, a Na^+ ionophore capable to collapse Na^+ and H^+ gradients [39], induces a significant pHi increase with respect to untreated cells, while monensin plus ANP

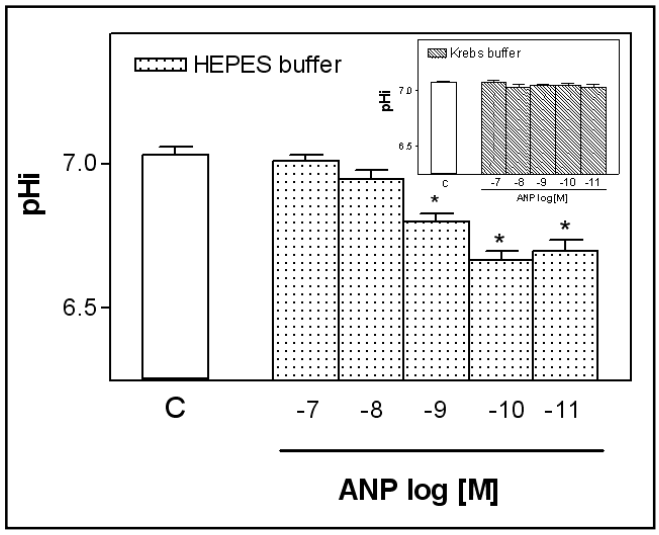

Fig. 1. ANP effects on pHi in HepG2 cells. HepG2 cells ($1x10^6$) were grown in RMPI-1640 plus 10% FCS and serum starved for 24 h before each experiment to rule out possible interferences with cell growth due to serum components and to promote their synchronization. Cells were adapted to HEPES or Krebs buffers for at least 5 hours before each experiment. Cells were challenged with a wide range of ANP concentrations (10^{-7}-10^{-11}M) in either HEPES or Krebs buffer (*inset*) for 6 hours and analyzed for pHi changes, as reported in Materials and Methods. Data are reported as mean ± SD of 4 different experiments. *P<0.05, as from a Student's t test, with respect to untreated cells (C).

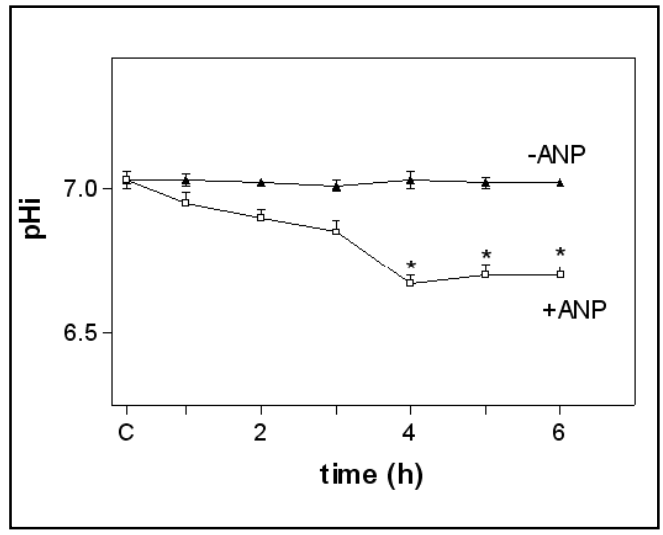

Fig. 2. Time-course of ANP effects on pHi in HepG2 cells. HepG2 cells ($1x10^6$), grown as reported in Fig. 1 legend, were challenged with 10^{-10} M ANP in HEPES buffer for different experimental times (1-6 hours) and pHi evaluated as described in Materials and Methods. Data are reported as mean ± SD of 4 different experiments. *P<0.05, as from a Student's t test, with respect to time 0 (C).

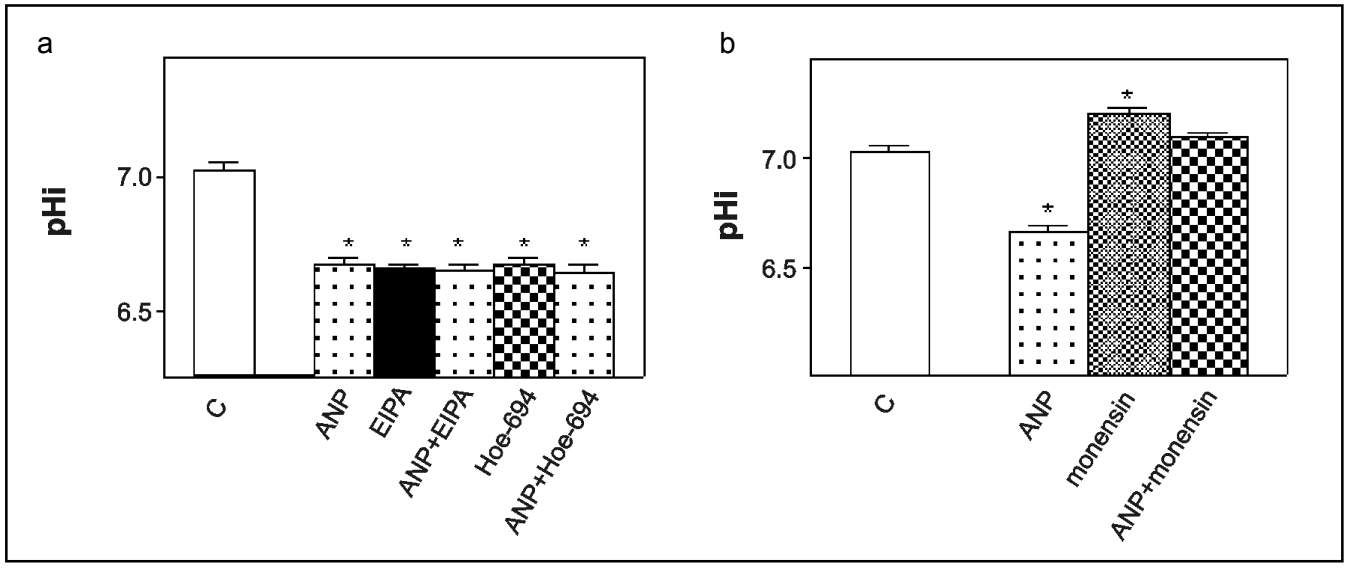

Fig. 3. ANP effects on pHi in the presence of NHE-1 inhibitors and monensin in HepG2 cells. HepG2 cells ($1x10^6$), grown as reported in Fig.1 legend, were challenged with 10^{-10}M ANP in HEPES buffer for 6 hours in the presence or absence of 1μM EIPA or 10μM Hoe-694 (a) and 10μM monensin (b) and analyzed for pHi changes as reported in Materials and Methods. Data are reported as mean ± SD of 4 different experiments. *P<0.05, as from a Student's t test, with respect to untreated cells (C).

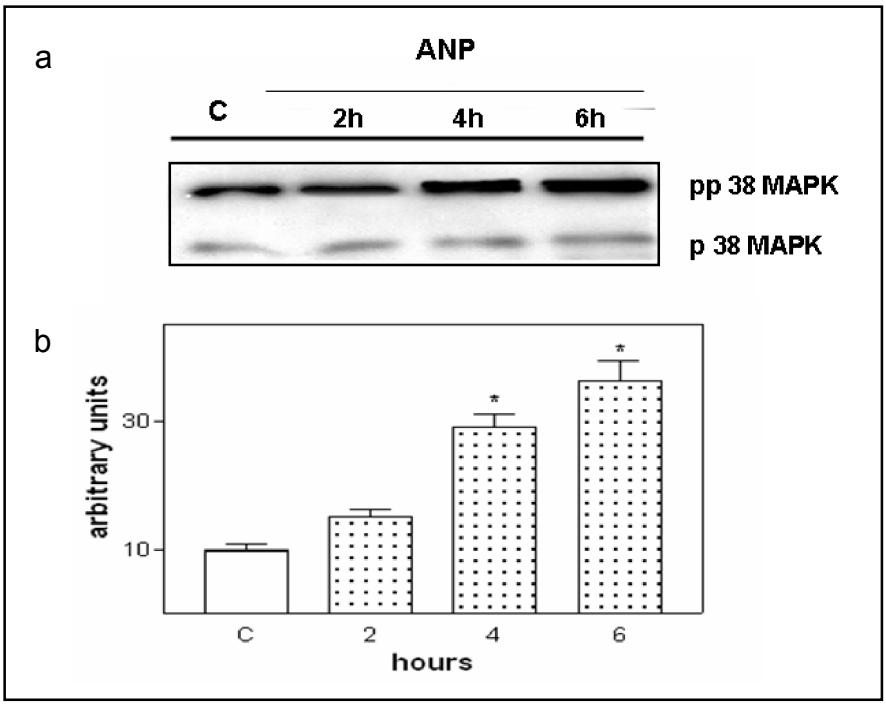

Fig. 4. ANP effects on p38 MAP kinase activation in HepG2 cells. (a) Cell lysates prepared from HepG2 cells were separated by SDS–PAGE. Immunoblotting was performed as described in Materials and Methods. Each lane represents lysates from HepG2 cells challenged with 10^{-10}M ANP for different experimental times (2-4-6 hours) or not (C). The figure shows a representative experiment repeated three additional times with similar results. *Upper row*: phosphorylated p38 MAP kinase (pp38 MAPK). *Lower row:* total p38MAP kinase. (b) Densitometric evaluation of pp38 MAP kinase signal intensity of three different experiments. *P< 0.05 at least, with respect to total p38 expression.

inhibits the hormone effect on pHi. Taken together, these results suggest a possible involvement of NHE-1 in ANP-induced pHi decrease in HepG2 cells.

Since p38 MAPK plays a key role in the modulation of NHE-1 [16, 40], we evaluated (i) the ability of ANP to phosphorylate such kinase and (ii) the possible role of this enzyme in ANP-induced pHi decrease. Immunoblots showed that p38 MAPK was constitutively activated and a time-dependent increase was detected after exposure to ANP with respect to untreated cells, with a maximal activation after 6 hours (Fig.4). The involvement of p38 MAPK in ANP-dependent pHi decrease was investigated in the presence of either 5μM SB203580, a specific inhibitor of the enzyme, or 10μM SB202474, an inactive analogue, as a control. Our results showed that the pHi decrease was entirely reverted only in the presence of SB203580 (Fig.5), confirming the involvement of this kinase in the mechanism through which ANP induced pHi decrease in HepG2 cells.

To investigate whether the marked ANP effects on pHi was due to a decreased NHE-1 expression, we performed time-course experiments on mRNA NHE-1 expression and protein levels in HepG2 cells treated or not with ANP (Fig. 6a,b,c). ANP significantly decreased mRNA NHE-1 expression already at 4 hours, while no significant differences were present between 4 and 6 hours treatment; these effects were totally inhibited in

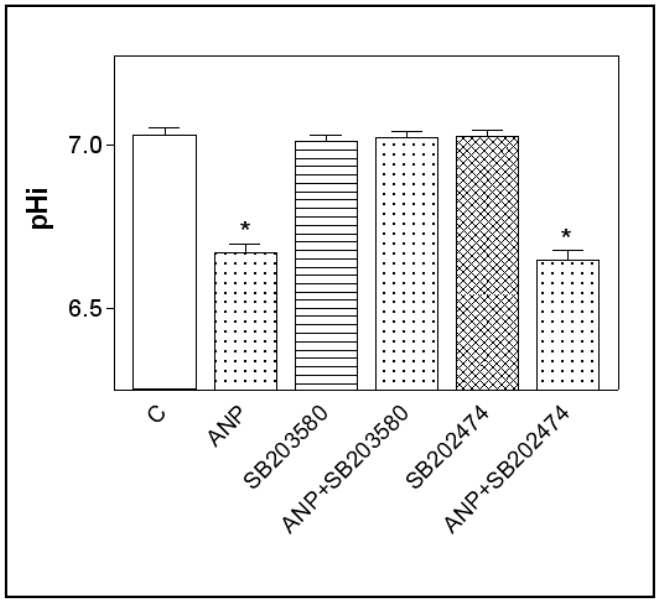

Fig. 5. ANP effects on pHi in the presence of SB203570 and SB202474 in HepG2 cells. HepG2 cells ($1x10^6$), grown as reported in Fig.1 legend, were challenged with 10^{-10}M ANP for 6 hours in the presence or absence of 5μM SB203580 or SB202474 and analyzed for pHi changes, as reported in Materials and Methods. Data are reported as mean ± SD of 4 different experiments. *P<0.05, as from a Student's t test, with respect to untreated cells (C).

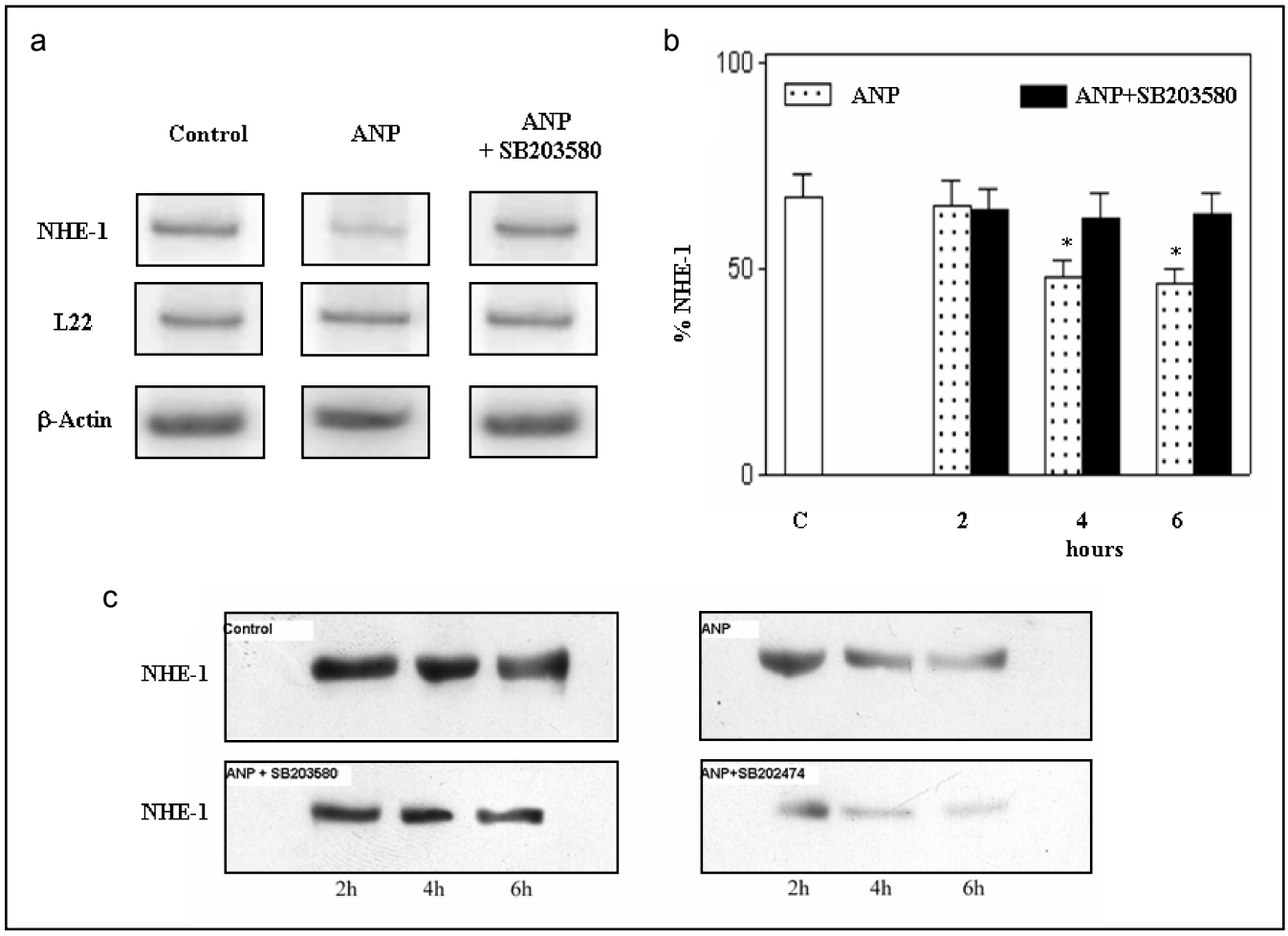

Fig. 6. Time-course of ANP effects on NHE-1 mRNA expression and protein level in HepG2 cells. Radioactive RT-PCR analysis was performed to amplify NHE-1 mRNA from HepG2 cells, as reported in Materials and Methods. (a) Representative experiment of total RNA isolated from HepG2 cells untreated (*Control*) or challenged with 10^{-10} M ANP or with ANP plus 5μM SB203580 for 6 hours and RT-PCR amplified in unsaturated condition with primers specific for NHE-1, L22 or β-actin mRNAs. (b) Cells were challenged for 2-4-6 hours with ANP in the presence or absence of SB203580. Five independent experiments were performed. NHE-1 signals were quantified and corrected vs. L22 mRNA and β-actin mRNA and reported as percentage. Values represent the mean ± SEM. * P<0,01, as from Student's t test, for ANP treated cells with respect to untreated cells (C). (c) Immunoblotting was performed as described in Materials and Methods. Each lane represents lysates from HepG2 cells treated with 10^{-10}M ANP or ANP plus 5μM SB203580 for different experimental times (2-4-6 hours). The figure shows a representative experiment repeated three additional times with similar results.

the presence of 5μM SB203580 (Fig.6 a,b). In addition, ANP was also able to decrease protein levels of NHE-1 (Fig. 6c). Such an effect was counteracted by SB203580, suggesting a key role of this enzyme in the down-regulation of ANP-induced NHE-1 expression.

Phosphatidylethanol (PetOH) production after intracellular acidification

Changes in pHi observed in response to an array of ligands may be considered signaling events for the activation of downstream effectors including phospholipases [20]. We investigated a possible relationship between pHi and phospholipase D (PLD) activity by the transphosphatidylation reaction, which catalyses, in the presence of ethanol, the phosphatidylethanol (PetOH) formation [36]. In Fig.7a, the time-course of ANP-induced PetOH production in HepG2 cells is reported; it shows: (i) in HEPES buffer: a

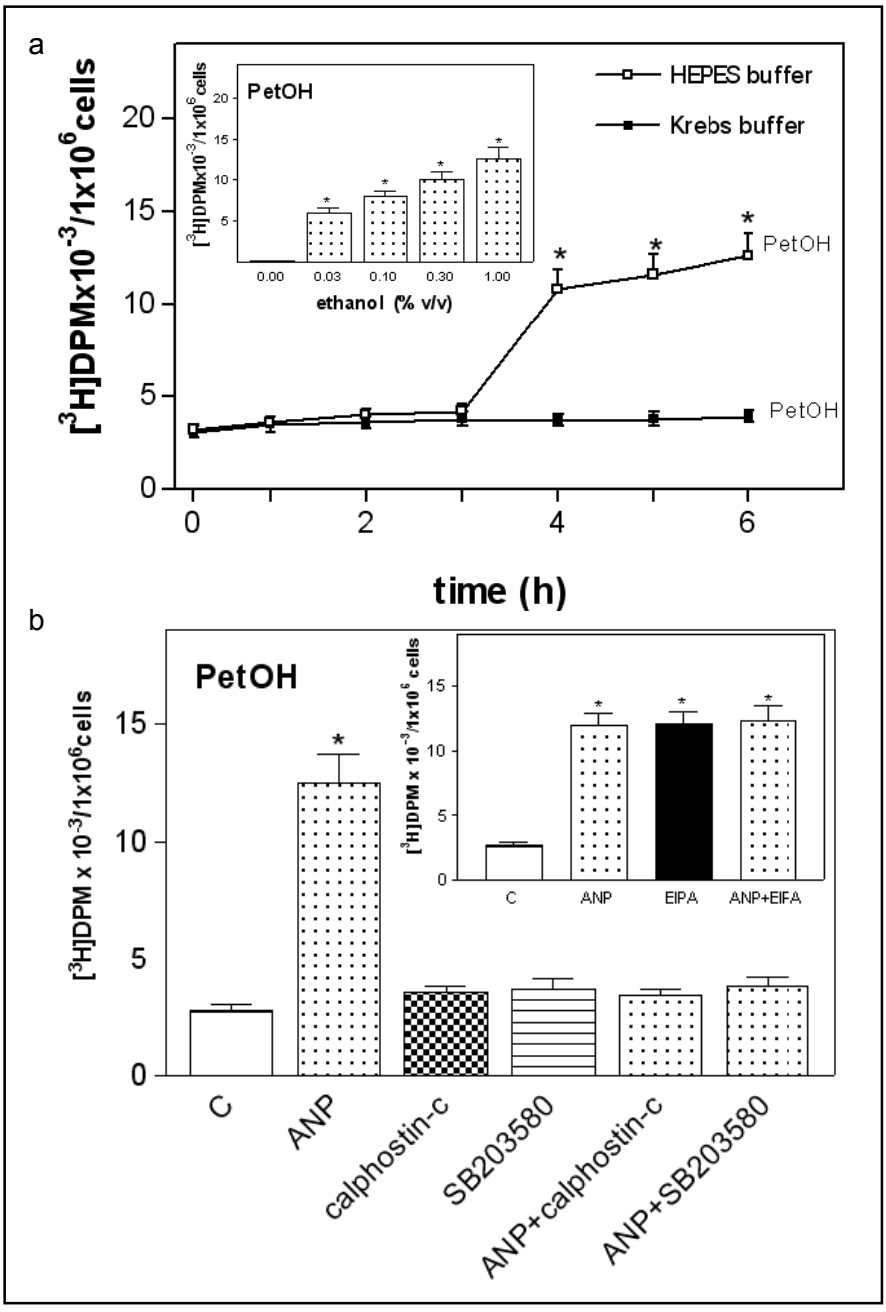

Fig. 7. ANP effects on [^{3}H] myristate incorporation into PetOH in HepG2 cells. (a) HepG2 cells ($1x10^6$) were labeled with [^{3}H]-myristic acid (1μCi) for 3 hours at 37°C before the addition of 10^{-10}M ANP for different experimental times (1-6 hours) in either HEPES or Krebs buffer, and PetOH production assessed as described in Materials and Methods. Data are reported as mean ± SD of 4 different experiments. *P<0.05, as from a Student's t test, with respect to time 0 (C). *Inset,* ANP effects on PetOH production in the presence of different ethanol concentrations. (b) HepG2 cells ($1x10^6$) were labeled with [^{3}H]-myristic acid (1μCi) for 3 hours at 37°C before the addition of 10^{-10}M ANP for 6 hours. 10^{-8}M calphostin-c and 5μM SB203580 were added 1 hour before ANP treatment and PetOH production assessed as reported in Materials and Methods. *Inset*, ANP effects on PetOH production in the absence or presence of 1μM EIPA. Data are reported as mean ± SD of 4 different experiments. *P<0.05, as from a Student's t test, with respect to untreated cells (C).

significant time-dependent increase in PetOH production after 4 hours treatment, while no significant differences were present between 4 and 6 hours; (ii) no significant ANP-induced PetOH increase was obtained in Krebs buffer (Fig.7a) as well as in HEPES buffer after adding monensin (data not shown). Changes in the concentration of short-chain primary alcohols, such as ethanol, represent a method to inhibit PLD-mediated production of PetOH by the transphosphatidylation reaction [36]. In Fig. 7a, *inset,* we report the dose-response curve of PetOH production in HepG2 cells incubated with different ethanol concentrations (0.03-1% v/v) before the exposition to ANP for 6 hours. In this regard, we observed a significant ethanol concentration-dependent increase in PetOH production after ANP stimulation, suggesting that PLD may represent a downstream target for the hormone. Since ethanol can modify pHi in hepatocytes [41], we monitored ANP effects on pHi in the presence of different ethanol concentrations and no significant differences were observed (data not shown). Therefore, we carried out experiments to evaluate PetOH production after ANP exposure in the presence of 10^{-8}M calphostin c, a potent inhibitor of PLD, or 5μM SB203580. Results, reported in Fig.7b, suggested that: (i) ANP induced a significant

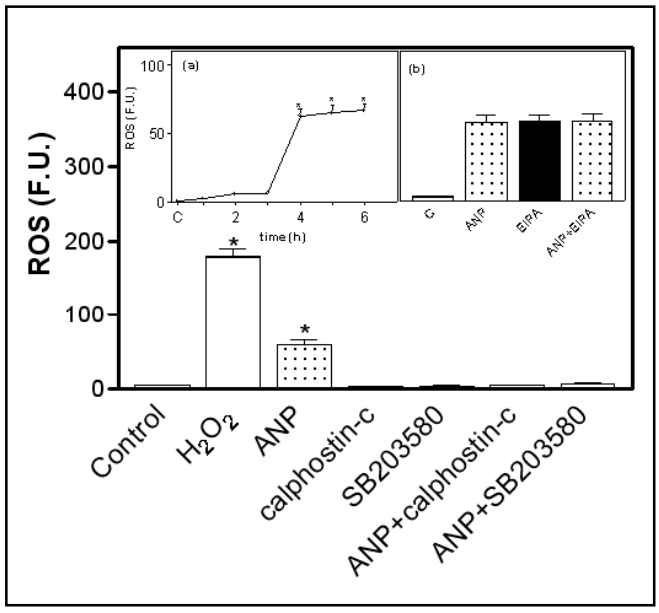

Fig. 8. ANP effects on ROS production in HepG2 cells. HepG2 cells were labeled with DCF-DA and ROS production was evaluated after 6 hours treatment with 10^{-10}M ANP as reported in Materials and Methods. 10^{-8}M calphostin-c and 5μM SB203580 were added 1 hour before ANP treatment. Results are expressed as Fluorescence Intensity, reported as Fluorescence Units (F.U.), of cells loaded with DCF-DA only (C) or also treated with 300 μM H_2O_2 for 1 hour as positive control. Data represent the mean ± SD values of 4 experiments. *P<0.05, as from a Student's t test, with respect to untreated cells (Control). *Inset a,* time-course of ANP-induced ROS production in HEPES buffer. *P<0.05, as from a Student's t test, with respect to time 0 (C). *Inset b*, ANP effects on ROS production in the absence or presence of 1μM EIPA.

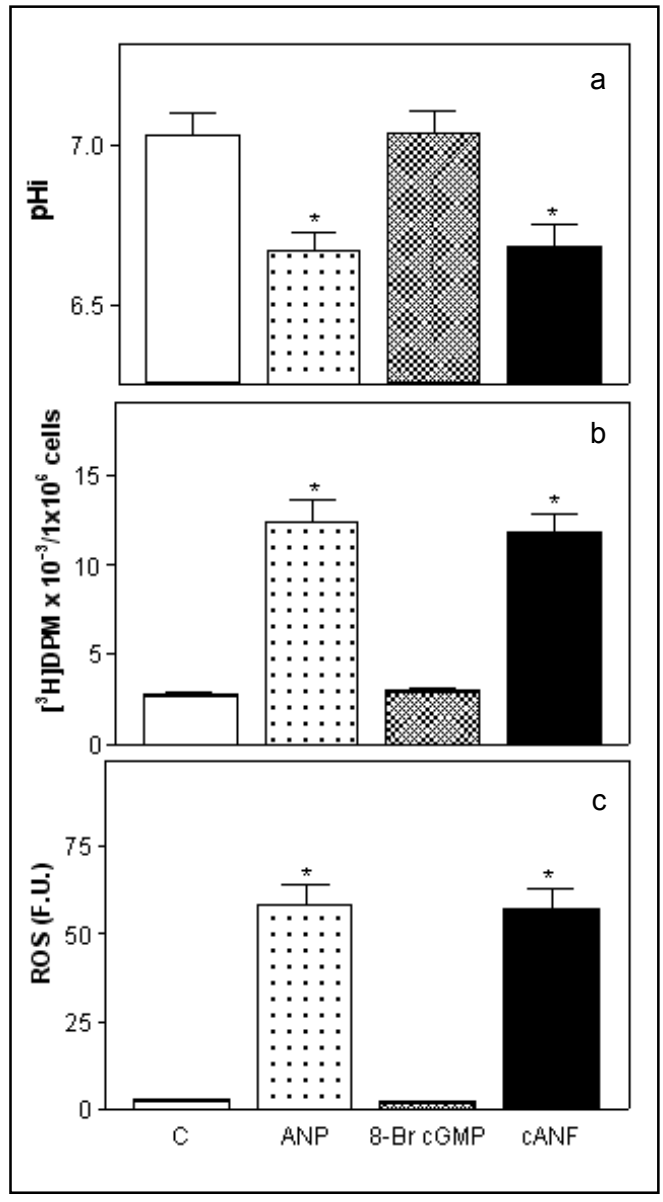

Fig. 9. 8-Br-cGMP and cANF effects on pHi, PetOH and ROS production. HepG2 cells, treated as reported in Fig. 2, 5 and 6 legends, were challenged with 10^{-10}M ANP, 10^{-10}M cANF and 50μM 8-Br-cGMP for 6 hours. pHi (a), PetOH (b) and ROS production (c) were assessed as reported in Materials and Methods. Data are the mean ± SD of 4 different experiments carried out in triplicate. *P<0.05, as from a Student's t test with respect to untreated cells (C).

increase in PetOH production with respect to untreated cells; (ii) 10^{-8} M calphostin-c or 5μM SB203580 alone were uneffective, while a total inhibition of the ANP effect was observed after pretreatment with SB203580 as well as calphostin-c. Fig. 7b, *inset*, shows that EIPA was able to mimic ANP effects on PetOH production and no additive effects were present with ANP plus EIPA. Experiments carried out in Krebs buffer showed no significant ANP effects on PetOH production (data not shown), suggesting a possible relationship between ANP-induced intracellular acidification and PLD activity in HepG2 cells.

PLD activity and Reactive Oxygen Species (ROS) production

Since PA enhances ROS production in several cell types [42], we examined the interplay between ANP-induced PLD activation and ROS production in HepG2 cells. In Fig.8, *inset a*, the time-course of ANP-induced ROS production in HEPES buffer shows a significant

time-dependent increase in ROS production after 4 hours treatment, while no significant differences were present between 4 and 6 hours.

Experiments carried out in the presence or absence of calphostin-c in HepG2 cells after 6 hours stimulation with ANP in HEPES buffer showed that (Fig.8): (i) ANP induced a significant increase in ROS production with respect to untreated cells; (ii) calphostin c alone did not affect ROS production, while the pretreatment with the inhibitor totally abrogated ANP-induced ROS production; (iii) similar results were obtained in the presence of SB203580. Finally, Fig. 8, *inset b*, shows that EIPA was able to mimic ANP effects on ROS production and no additive effects were present with ANP plus EIPA. Taken together, these results suggest a possible link among ANP-induced intracellular acidification, phospholipase D activation and ROS production with the involvement of p38 MAP kinase.

Selectivity of ANP receptors in HepG2 cells

The potential role of ANP-receptors in the above reported hormone-induced effects was investigated. We carried out experiments with 8-Br-cGMP, a non hydrolysable analogue of cGMP involved in ANP effects mediated by NPR-A receptors, and cANF (4-23), the ring–deleted analogue of ANP acting as specific activator of NPR-C receptors. Fig. 9 shows that 10^{-10} M cANF was able to mimic ANP-induced effects on pHi (a), PLD activation (b) and ROS production (c), while 50 μM 8-Br-cGMP was ineffective, suggesting the involvement of NPR-C receptors in the hormone action.

Discussion

Cellular ionic events, such as changes in transmembrane electric potential, Na^+ and Ca^{++} intracellular concentrations and intracellular pH, are necessary to regulate cell functions. Several transport systems are involved in pHi homeostasis. One of the best described is NHE-1, a plasma membrane protein, which plays a regulative role being activated by hormones and growth factors [15]. In several tumors, the extracellular microenvironment is more acidic than normal tissues; in these conditions, the NHE-1 exchanger represents the only system able to regulate pHi homeostasis. The early activation of NHE-1 is also considered as an important event in cell proliferation and malignant transformation [43]. Conversely, ANP contributes to cell growth modulation by eliciting an antiproliferative action in different cell types. In hepatocellular carcinoma and HepG2 cells, an increased expression of ANP can decrease cell growth by NPR-C downregulation [11] and NHE-1 mRNA levels and the exchanger activity are 10 and 3 fold higher than in normal hepatocytes, respectively [27, 28]. These features prompted us to consider this cell type to investigate on possible effects of ANP on intracellular acidification. Our results show that, in HepG2 cells, ANP effects on pHi were present only at peptide concentrations as low as 10^{-10} M, i. e. within the physiological range of ANP plasma concentrations, the missed response to higher concentrations being determined by a possible NPR-A receptor downregulation due to long- term effects of ANP [44], as already suggested in human macrophages [22]. Remarkably, these results were obtained in HEPES buffer to more closely mimic the acidic environmental conditions typical of malignant cells, in which NHE-1, represents the only system involved in pHi homeostasis [43].

ANP can early regulate pHi through NHE-1 [12, 13, 34]. In fact, pharmacological concentrations of the hormone inhibit NHE-1 by a mechanism that includes increased intracellular levels of cGMP, while physiological concentrations can stimulate NHE-1 through the diacylglycerol production or cAMP decrease [13]. Kusuhara et al. [16] showed that p38 MAPK is able to induce an early decrease NHE-1 activity proposing two possible mechanisms. First, p38 MAPK may phosphorylate NHE-1, causing a conformational change that inhibits the transport activity; second, the kinase may decrease the p42/44 MAPK activity responsible for the inhibition of downstream effectors, such as NHE-1 kinases. Our observations show that the ANP-induced pHi decrease in HepG2 cells involves the phosphorylation of p38 MAPK leading to the downregulation of NHE-1 mRNA and protein levels, suggesting a key role for p38 MAPK as upstream effectors for ANP signaling pathways.

Changes in pHi induced by a variety of biologically active molecules, such as ANP, may act as signaling event for the regulation of downstream effectors including phospholipase D [20, 22]. In this respect, in HepG2 cells, ANP induces a significant increase in PetOH intracellular levels through PLD activation, as also confirmed by the treatment with calphostin-c, a potent inhibitor of the enzyme [33]. Since PLD activation can be enhanced when NHE-1 is inhibited [20], experiments were carried out in the presence of EIPA, to inhibit NHE-1 exchanger: the inhibitor was able to mimic ANP effects on PLD activity, suggesting interplay between pHi and ANP-

induced PLD activation. Moreover, the hormone effects on pHi and PLD activation were also inhibited by SB203580, an inhibitor of p38 MAPK, confirming a significant role of this kinase as downstream effector of ANP signaling pathways.

In HepG2 cells [26, 45], different agonists can induce ROS production which can play a role as mediator of cell death. Here, we show that changes in pHi exhibited in response to physiological concentrations of ANP can be responsible for ROS production through the activation of p38 MAPK and PLD. Since experimental evidences [46] describe the ability of ANP to inhibit cell growth, our data support the possibility that ROS production may be involved in the mechanism by which ANP inhibits HepG2 cell growth, by necrosis [47]

Finally, our findings appear partially in disagreement with previous reports showing the ANP ability to reduce liver ischemia/reperfusion injury and improving hepatocytes resistance to oxidative stress [48]. It should not be surprising that ANP elicits different effects. In fact, hormone effects can be determined through different pathways depending on the phenotypic state of cells [49]. In particular, cells which undergo phenotypic modulation express a relatively high number of NPR-C receptors and are highly sensitive to ANP [49]. In hepatoblastoma cells, the ability of ANP to inhibit proliferation has been attributed to the selective upregulation of C-ANP receptor expression [11]. Since all biological effects assessed in this study were due to physiological concentrations of ANP and, at the same time, NHE-1 inhibition was related to cell proliferation, we speculate that the NPR-C receptor upregulation can be involved in ANP effects on HepG2 cells. Interestingly, our results show that cANF, the NPR-C specific ring deleted analogue of ANP, is able to mimic ANP-induced effects on pHi, PLD activity and ROS production demonstrating, for the first time, an important role for NPR-C receptors in ANP-induced ROS production.

References

1 Brenner BM, Ballerman BJ, Gunning ME, Ziedel ML: Diverse biological actions of atrial natriuretic peptide. Physiol Rev 1990;70:665-699.

2 Rubattu S, Volpe M: The atrial natriuretic peptide: a changing view. J Hypertens 2001;19:1923-1931.

3 Berk BC: Vascular smooth muscle growth. Autocrine growth mechanisms. Physiol Rev 2001;81:999-1030.

4 Eiskjaer H, Nielsen CB, Pedersen EB: Pressure-dependent distal tubular action of atrial natriuretic peptide in healthy humans. J Hypertens 1996;14:99-106.

5 Zhao L, Mason NA, Strange JW, Walker H, Wilkins MR: Beneficial effects of phosphodiesterase 5 inhibition in pulmonary hypertension are influenced by natriuretic peptide activity. Circulation 2003;107:234-237.

6 Vollmar AM: Influence of atrial natriuretic peptide on thymocyte development in fetal thymic organ culture. J Neuroimmunol 1997;78:90-96.

7 Bilzer M, Witthaut R, Paumgartner G, Gerbes AL: Prevention of ischemia/reperfusion injury in the rat liver by atrial natriuretic peptide. Gastroenterology 1994;106:43-51.

8 Vollmar AM, Paumgartner G, Gerbes AL: Differential gene expression of the three natriuretic peptides and natriuretic peptide receptor subtypes in human liver. Gut 1997;40:145-150.

9 Anand-Srivastava MB,Trachte GJ: Atrial Natriuretic Factor receptors and signal transduction mechanisms. Pharmacol Rev 1993;45:455-497.

10 Zannetti A, Luly P, Musanti R, Baldini PM: Phosphatidylinositol-and phosphatidylcholine-dependent phospholipase C are involved in the mechanism of action of atrial natriuretic factor in cultured rat aortic smooth muscle cells. J Cell Physiol 1997;170:272-278.

11 Rashed HM, Sun H, Patel TB: Atrial natriuretic peptide inhibits growth of hepatoblastoma (HEPG2) cells by means of activation of clearance receptors. Hepatology 1993;17:677-684.

12 Kanda F, Sarnacki P, Arieff AI: Atrial natriuretic peptide inhibits amiloride-sensitive sodium uptake in rat brain. Am J Physiol 1992;263:R279-R283.

13 Ricci R, Baldini P, Boggetto L, De Vito P, Luly P, Zannetti A, Incerpi S: Dual modulation of Na/H antiport by atrial natriuretic factor in rat aortic smooth muscle cells. Am J Physiol 1997;273:C643-C652.

14 Horvat B, Taheri S, Salihagic A: Tumour cell proliferation is abolished by inhibitors of Na^+/H^+ and HCO_3^-/Cl^- exchange. Eur J Cancer 1993;29:132-137.

15 Wakabayashi S, Shigekawa M, Pouyssegur J: Molecular physiology of vertebrate Na^+/H^+exchangers. Physiol Rev 1997;77:51-74.

16 Kusuhara M, Takahashi E, Peterson TE, Abe J, Ishida M, Han J, Ulevitch R, Berk BC: p38 kinase is a negative regulator of angiotensin II signal transduction in Vascular Smooth Muscle cells. Effects on Na^+/H^+ exchange and ERK1/2. Circ Res 1998;83:824-831.

17 Pearson G, Robinson F, Gibson TB, Xu B, Karandikar M, Berman K,Cobb MH: Mitogen-activated protein (MAP) kinase pathways: regulation and physiological functions. Endocrine Reviews 2001;22:153-183.

18 Tsukagoshi H, Shimizu Y, Kawata T, Hisada T, Shimizu Y, Iwamae S, Ishizuka T, Iizuka K, Dobashi K, Mori M: Atrial natriuretic peptide inhibits tumor necrosis factor-alpha production by interferon-gamma-activated macrophages via suppression of p38 mitogen-activated protein kinase and nuclear factor-kappa B activation. Regul Pept 2001;99:21-29.

19 Kiemer AK, Kulhanek-Heinze S, Gerwig T, Gerbes AL, Vollmar AM: Stimulation of p38 MAPK by hormonal preconditioning with atrial natriuretic peptide. World J Gastroenterol 2002;8:707-711.

20 Gewirtz AT, Seetoo KF, Simons ER: Neutrophil degranulation and phospholipase D activation are enhanced if the Na^+/H^+ antiport is blocked. J Leukoc Biol 1998;64:98-103.

21 Baldini PM, Incerpi S, Zannetti A, De Vito P, Luly P: Selective activation by atrial natriuretic factor of phosphatidylcholine-specific phospholipase activities in purified heart muscle plasma membranes. J Mol Cell Cardiol 1994;26:1691-1700.
22 Baldini PM, De Vito P, Martino A, Fraziano M, Grimaldi C, Luly P, Zalfa F, Colizzi V: Differential sensitivity of human monocytes and macrophages to ANP: a role of intracellular pH on reactive oxygen species production through the phospholipase involvement. J Leukoc Biol 2003;73:502-510.
23 Exton JH: Phospholipase D-structure, regulation and function. Rev Physiol Biochem Pharmacol 2002;144:1-94.
24 Gomez-Cambronero J, Keire P: Phospholipase D: a novel major player in signal transduction. Cell Signal 1998;6:387-397.
25 Cummings R, Parinandi N, Wang L, Usatyuk P, Natarajan V: Phospholipase D/phosphatidic acid signal transduction: role and physiological significance in lung. Mol Cell Biochem 2002;234:99-109.
26 Lee YS, Kang YS, Lee SH, Kim JA: Role of NAD(P)H oxidase in the tamoxifen-induced generation of reactive oxygen species and apoptosis in HepG2 human hepatoblastoma cells. Cell Death Differ 2000;7:925-932.
27 Ananthanarayanan M, Reilly RF, Igarashi P, Suchy FJ: Enhanced transcript levels for the Na/H exchanger during development of rat liver and in hepatoma cells. Hepatology 1991;14:418.
28 Weintraub WH, Machen TE: pH regulation in hepatoma cells: roles for Na^-H exchange, Cl^-/HCO_3^- exchange and $Na^- HCO_3$ cotransport. Am J Physiol 1989;257:317-G327.
29 Grinstein S, Cohen S, Goetz-Smith JD, Dixon SJ: Measuraments of cytoplasmatic pH and cellular volume for detection of Na^+/H^+ exchange in lymphocytes. Methods Enzymol 1989;173:777-779.
30 Thomas JA, Buchsbaum RN, Zimniak A, Racker E: Intracellular pH measurements in Ehrlich ascites tumor cells utilizing spectroscopic probes generated in situ. Biochemistry 1979;18: 2210-2218.
31 Lowry OH, Rosebrough NJ, Farr AL, Randall RJ: Protein measurement with the Folin phenol reagent. J Biol Chem 1951;193:265-268.
32 Chomczynski P, Sacchi N: Single-step method of RNA isolation by acid guanidinium thyocianate-phenol-chloroform extraction. Anal Biochem 1987;162:156-159.
33 Sciorra VA, Hammond SM, Morris AJ: Potent direct inhibition of mammalian phospholipase D isoenzymes by calphostin-c. Biochemistry 2001;40:2640-2646.
34 Ping P, Murphy E: Role of p38 mitogen-activated protein kinases in preconditioning a detrimental factor or a protective kinase? Circ Res 2000;86:921-922.
35 Bligh EG, Dyer WJ: A rapid method of total lipid extraction and purification. Can J Biochem 1959;37:911-917.
36 Shukla SD, Halenda SP: Phospholipase D in cell signalling and its relationship to phospholipase C. Life Sci 1991;48:851-866.
37 Chattopadhyay J, Natarajan V, Schmid HH: Membrane-associated phospholipase D activity in rat sciatic nerve. J Neurochem 1991;57:1429-1436.
38 Shen HM, Shi CY, Shen Y, Ong CN: Detection of elevated reactive oxygen species level in cultured rat hepatocytes treated with aflatoxin B1. Free Radic Biol Med 1996;21:139-146.
39 Pressman BC: Biological application of ionophores. Ann Rev Biochem 1976;45:501-530.
40 Khaled AR, Moor AN, Li A, Kim K, Ferris DK, Muegge K, Fisher RJ, Fliegel L, Durum SK: Trophic factor withdrawal: p38 mitogen-activated protein kinase activates NHE1, which induces intracellular alkalinization. Mol Cell Biol 2001;21:7545-7557.
41 Kubitz R, D'Urso D, Keppler D, Haussinger D: Osmodependent dynamic localization of the mrp2 gene-encoded conjugated export pump in the rat hepatocyte canalicular membrane. Gastroenterology 1997;113:1438-1442
42 Palicz A, Foubert TR, Jesaitis AJ, Marodi L, McPhail LC: Phosphatidic acid and diacylcglycerol directly activate NADPH oxidase by interacting with enzyme components. J Biol Chem 2001;276:3090-3097.
43 Reshkin SJ, Bellizzi A, Caldeira S, Albarani V, Malanchi I, Poignee M, Alunni Fabroni M, Casavola V, Tommasini M: Na^+/H^+ exchanger-dependent intracellular alkalinization is an early event in malignant transformation and plays an essential role in the development of subsequent transformation- associated phenotypes. FASEB J 2000;14:2185-2197.
44 Cao L, Wu J, Gardner DG: Atrial natriuretic peptide supresses the transcription of its guanylyl cyclase- linked receptor. J Biol Chem 1995;270:24891-24897.
45 Kim J, Lee YS: Role of reactive oxygen species generated by NADPH oxidase in the mechanism of activation of K^+-Cl^- cotransport by N-ethylmaleimide in HepG2 human hepatoma cells. Free Rad Res 2001;35:43-53.
46 Silberbach M, Roberts CT Jr:Natriuretic peptide signaling. Molecular and cellular pathways to growth regulation. Cell Signal 2001;13:221-231
47 Baldini PM, De Vito P, Antenucci D, Vismara D, D'Aquilio F, Luly P, Zalfa F, Bagni C, Di Nardo P: Atrial Natriuretic Peptide induces cell death in human hepatoblastoma (HepG2) through the involvement of NADPH oxidase.Cell Death Differ (in press)
48 Carini R, De Cesaris MG, Splendore R, Domenicotti C, Nitti MP, Pronzato MA, Albano E: Mechanisms of hepatocyte protection against hypoxic injury by atrial natriuretic peptide. Hepatology 2003;37:277-285.
49 Cahill PA, Hassid A: ANF-C receptor-mediated inhibition of aortic smooth muscle cell proliferation and thymidine kinase activity. Am J Physiol 1994;266:R194-R203.